

JAERI-M
92-057

NUMERICAL ANALYSIS OF GAS PUFF MODULATION EXPERIMENT ON JT-60U

March 1992

Keisuke NAGASHIMA and Akira SAKASAI

JAERI Mレポートは、日本原子力研究所が不定期に公開している研究報告書です。

入手の間合わせは、日本原子力研究所技術情報部情報資料課 〒319-11茨城県那珂郡東海村 まで、お申しこみください。なお、このほかにも財団法人原子力弘済会資料センター 〒319-11茨城県那珂郡東海村日本原子力研究所内）で複写による実費領布をおこなっております。

JAERI M reports are issued irregularly.

Inquiries about availability of the reports should be addressed to Information Division Department of Technical Information, Japan Atomic Energy Research Institute, Tokaimura, Naka gun, Ibaraki ken 319-11, Japan.

© Japan Atomic Energy Research Institute, 1991

編集兼発行者 日本原子力研究所
印刷 ニッセイエプロ株式会社

Numerical Analysis of
Gas Puff Modulation Experiment on JT-60U

Keisuke NAGASHIMA and Akira SAKASAI

Department of Fusion Plasma Research
Naka Fusion Research Establishment
Japan Atomic Energy Research Institute
Naka-machi, Naka-gun, Ibaraki-ken

(Received March 13, 1992)

In tokamak transport physics, source modulation experiments are one of the most effective methods. For an analysis of these modulation experiments, a simple numerical method was developed to solve the general transport equations. This method was applied to gas puff modulation experiments on JT-60U. From the comparison between the measured and calculated density perturbations, it was found that the particle diffusion coefficient is about $0.8 \text{ m}^2/\text{sec}$ in the edge region and $0.1\text{-}0.2 \text{ m}^2/\text{sec}$ in the central region.

Keywords: Tokamak, Transport Physics,
Particle Diffusion Coefficient Modulation Experiment, JT-60U,

JT-60Uにおけるガスパフ振動実験の数値的解析

日本原子力研究所那珂研究所炉心プラズマ研究部

永島 圭介・逆井 章

(1992年3月13日受理)

トカマクの輸送物理において、ある種の入力源を振動させることによってその応答を測定する実験は、最も有効な実験のひとつとなっている。こうした振動実験の解析のために、一般的な輸送方程式を解くための簡易な方法を考案した。更に、JT-60Uにおけるガスパフ振動実験にこの方法を適用した。測定及び計算から得られた密度の変動分を比較することにより、粒子拡散係数は、プラズマ周辺部で $0.8\text{m}^2\text{sec}$ 、中心部で 0.1 から $0.2\text{m}^2\text{sec}$ 程度であることが明らかになってきた。

Contents

1. Introduction	1
2. Numerical Method	1
3. Application to Gas Puff Modulation Experiments	5
4. Conclusion	7
Acknowledgements	7
References	7

目 次

1. 序 論	1
2. 数値的解法	1
3. ガスパフ振動実験への適用	5
4. 結 論	7
謝 辞	7
参考文献	7

1. Introduction

In fusion plasma experiments, the physics of heat and particle transports is one of the most important problems and is not fully understood until now. Especially, in tokamak plasmas, many experiments have been performed to determine the local transport coefficients, as the particle and heat diffusion coefficients, D and χ . In these experiments, source modulation methods are popular and effective, and many kinds of sources have been used to analyze the response of the corresponding plasma parameter. For example, the response of the electron temperature was analyzed using modulation of additional heating power¹⁾, and the electron and impurity densities were analyzed using modulations of working gas and of impurity injection^{2,3)}. In some of these experiments, the obtained values of the local transport coefficients were different from the values determined from the steady state analysis of the particle and heat balances¹⁾. This discrepancy is an important problem to understand the tokamak transport phenomena⁴⁾.

In source modulation experiments, the measured data was analyzed using analytical solution of the diffusion equation³⁾, which was solved assuming that the transport coefficients are spatially constant and/or the source term is negligible. However, in some experiments, these assumptions is not valid. For example, in a gas puff modulation experiment²⁾, the measured density includes the effect of the edge source region, if one uses an interferometer as a diagnostic tool. Therefore, in this case, the particle source profile should be taken into account in the analysis. To include these effects, numerical calculation of the original equations is appropriate. But, the full time dependent calculation needs much calculation time. Therefore, we developed a simple numerical method to analyze the general transport equations for source modulation experiments.

In this paper, we will describe the developed numerical method in Sec.II and the application to gas puff modulation experiments on JT-60U in Sec.III. Lastly, a brief conclusion will be given.

2. Numerical Method

Here we consider the general form of a set of second order differential equations as follows

$$\frac{\partial z_i(x,t)}{\partial t} = \sum_j \widehat{L}_{ij}^2 z_j(x,t) + S_i(x,t) \quad (1)$$

$$\widehat{L}_{ij}^2 \equiv a_{ij}(x) \frac{\partial^2}{\partial x^2} + b_{ij}(x) \frac{\partial}{\partial x} + c_{ij}(x) \quad (2)$$

where \widehat{L}_{ij}^2 represents a second order differential operator that operates on the j -th function $z_j(x,t)$ in the i -th equation. $z_i(x,t)$ ($1 \leq i \leq I$) is a complex function with space and time parameters, x and t , and $S_i(x,t)$ is a source function. Eq.(1) represents the general form of the linearized transport equations and the functions $z_i(x,t)$ correspond to plasma parameters, as density, temperature and etc. We consider the case that all source functions $S_i(x,t)$ ($1 \leq i \leq I$) are modulated in a form of sinusoidal as $S_i(x,t) = S_i(x) \exp(i\omega t)$. Therefore, as response to the source modulation, all quantities $z_i(x,t)$ are modulated in the same form $z_i(x,t) = z_i(x) \exp(i\omega t)$ and Eq.(1) is written as

$$\sum_j \widehat{L}_{ij}^2 z_j(x) - i\omega z_i(x) + S_i(x) = 0 \tag{3}$$

where it is noted that $z_i(x)$ and $S_i(x)$ are both complex functions.

In general, a second order differential equation can be written as two first order differential equations. Here, we write I complex functions, $z_i(x)$ ($i \leq I$) as $4I$ real functions, y_i ($1 \leq i \leq 4I$) as follows

$$\mathbf{X} = \begin{pmatrix} X_1 \\ \cdot \\ X_i \\ \cdot \\ \cdot \\ X_I \end{pmatrix}, \quad \mathbf{X}_i = \begin{pmatrix} y_{4i-3} \\ y_{4i-2} \\ y_{4i-1} \\ y_{4i} \end{pmatrix} = \begin{pmatrix} \text{Re } z_i \\ \text{Re } z_i' \\ \text{Im } z_i \\ \text{Im } z_i' \end{pmatrix} \tag{4}$$

Eq.(3) can be written as a simple matrix equation with only first order derivatives.

$$\mathbf{A} \cdot \mathbf{X}' = \mathbf{B} \cdot \mathbf{X} - \mathbf{S} \tag{5}$$

where \mathbf{X}' represents $\partial \mathbf{X} / \partial x$. Matrices \mathbf{A} and \mathbf{B} are determined from the coefficients of Eq.(2) and \mathbf{S} is a vector corresponding to the source functions. Eq.(5) is rewritten by multiplying both sides by \mathbf{A}^{-1}

$$\mathbf{X}' = \mathbf{A}^{-1} \cdot \mathbf{B} \cdot \mathbf{X} - \mathbf{A}^{-1} \cdot \mathbf{S} \tag{6}$$

Eq.(6) is the general matrix equation that we consider in this section.

Here, to clarify the structure of Eqs.(4)-(6), we consider the most simple case of I=1 (only one function of z(x)). Eq.(3) is written as

$$\frac{\partial^2 z}{\partial x^2} + \alpha(x) \frac{\partial z}{\partial x} + \beta(x)z - i\hat{\omega}z + \hat{S}(x) = 0 \tag{7}$$

where it is noted that $\hat{\omega}$ and \hat{S} in Eq.(7) are different from ω and S in Eq.(3) by a factor of $a(x)$ (the coefficient of the second order derivative in Eq.(2)). Following Eq.(4), we define the functions of $y_i(1 \leq i \leq 4)$ as $y_1 = \text{Re } z$, $y_2 = \text{Re } \partial z / \partial x$, $y_3 = \text{Im } z$ and $y_4 = \text{Im } \partial z / \partial x$. Eq.(7) can be written as

$$\begin{pmatrix} \partial y_1 / \partial x \\ \partial y_2 / \partial x \\ \partial y_3 / \partial x \\ \partial y_4 / \partial x \end{pmatrix} = \begin{pmatrix} 0 & 1 & 0 & 0 \\ -\beta & -\alpha & -\hat{\omega} & 0 \\ 0 & 0 & 0 & 1 \\ \hat{\omega} & 0 & -\beta & -\alpha \end{pmatrix} \begin{pmatrix} y_1 \\ y_2 \\ y_3 \\ y_4 \end{pmatrix} - \begin{pmatrix} 0 \\ \text{Re } \hat{S} \\ 0 \\ \text{Im } \hat{S} \end{pmatrix} \tag{8}$$

This equation corresponds to Eq.(5) for I=1 (in this case, matrix **A** is the unit matrix).

Returning to Eq.(6), we rewritten it as

$$\mathbf{X}' = \mathbf{R} \cdot \mathbf{X} - \mathbf{P} \tag{9}$$

and define the matrix **F** as

$$\mathbf{F} \equiv \mathbf{R} \cdot \mathbf{X} - \mathbf{P} \tag{10}$$

We can obtain the algebraic equations of X_i ($0 \leq i \leq N$, N is a number of division in space region and it is noted that the subscript i is different from Eq.(4).) using the general numerical procedure as

$$X_{i+1} - X_{i-1} = \frac{h}{3} (F_{i+1} + 4F_i + F_{i-1}) \tag{11}$$

$$X_1 - X_0 = \frac{h}{2} (F_1 + F_0) \tag{12}$$

where h is an unit increment of the space parameter x . Using Eqs.(11) and (12), Eq.(9) can be written as

$$\mathbf{X}_{i+1} = \mathbf{A}_i \cdot \mathbf{X}_i + \mathbf{B}_i \cdot \mathbf{X}_{i-1} - \mathbf{S}_i \quad (13)$$

$$\mathbf{X}_1 = \mathbf{A}_0 \cdot \mathbf{X}_0 - \mathbf{S}_0 \quad (14)$$

and the matrices \mathbf{A}_i , \mathbf{B}_i and \mathbf{S}_i are defined as

$$\mathbf{A}_i = (\mathbf{I} - (h/3)\mathbf{R}_{i+1})^{-1} (4/3)h \mathbf{R}_i \quad (15)$$

$$\mathbf{B}_i = (\mathbf{I} - (h/3)\mathbf{R}_{i+1})^{-1} (\mathbf{I} + (h/3)\mathbf{R}_{i-1}) \quad (16)$$

$$\mathbf{S}_i = (\mathbf{I} - (h/3)\mathbf{R}_{i+1})^{-1} (h/3)(\mathbf{P}_{i+1} + 4\mathbf{P}_i + \mathbf{P}_{i-1}) \quad (17)$$

$$\mathbf{A}_0 = (\mathbf{I} - (h/2)\mathbf{R}_1)^{-1} (\mathbf{I} + (h/2)\mathbf{R}_0) \quad (18)$$

$$\mathbf{S}_0 = (\mathbf{I} - (h/2)\mathbf{R}_1)^{-1} (h/2)(\mathbf{P}_1 + \mathbf{P}_0) \quad (19)$$

where \mathbf{I} represents the unit matrix.

As the vector \mathbf{X}_i is linear with respect to the source matrix \mathbf{S}_i , we can rewrite \mathbf{X}_i as follows

$$\mathbf{X}_i = \mathbf{A}_{i-1} \cdot \mathbf{X}_{i-1} + \mathbf{B}_{i-1} \cdot \mathbf{X}_{i-2} - \mathbf{S}_{i-1} \equiv \mathbf{M}_i \cdot \mathbf{X}_0 - \sum_{j=0}^{i-1} \mathbf{N}_j^i \cdot \mathbf{S}_j \quad (20)$$

and the matrices \mathbf{M}_i and \mathbf{N}_j^i satisfy the following relations as

$$\mathbf{M}_i = \mathbf{A}_{i-1} \cdot \mathbf{M}_{i-1} + \mathbf{B}_{i-1} \cdot \mathbf{M}_{i-2} \quad (21)$$

$$\mathbf{N}_j^i = \mathbf{A}_{i-1} \cdot \mathbf{N}_j^{i-1} + \mathbf{B}_{i-1} \cdot \mathbf{N}_j^{i-2} \quad (0 \leq j \leq i-3) \quad (22)$$

$$\mathbf{N}_j^i = \mathbf{A}_{i-1} \cdot \mathbf{N}_j^{i-1} \quad (j=i-2) \quad (23)$$

$$\mathbf{N}_j^i = \mathbf{I} \quad (j=i-1)$$

Lastly, we define the total source matrix \mathbf{T}_i as follows

$$\mathbf{X}_i = \mathbf{M}_i \cdot \mathbf{X}_0 - \mathbf{T}_i, \quad \mathbf{T}_i \equiv \sum_{j=0}^{i-1} \mathbf{N}_j^i \cdot \mathbf{S}_j \quad (24)$$

To obtain a solution of this system, it is necessary that appropriate boundary conditions are used. In general, the boundary conditions are given at the edge of the calculated region (for example, $x=a$ and b) as the values of $z(a)$, $z(b)$ or $z(a)'$, $z(b)'$. In Eq.(24), the boundary conditions are given as the some values of the elements in X_0 and X_N . As the matrices M_i and T_i can be calculated from R_i and P_i , we obtain the full boundary conditions (the all values of the elements in X_0 and X_N) from the relation of $X_N=M_N X_0-T_N$. Once the values of X_0 are obtained, all values of X_i can be calculated from Eq.(24).

3. Application to Gas Puff Modulation Experiment:

Using the above mentioned numerical procedure, we analyzed gas puff modulation experiments on JT-60U. In these experiments, the injection of the working gas was modulated in a form of sinusoidal. As a result of this source modulation, the electron density was also modulated sinusoidally but with some phase delay. The aim of these experiments is to determine the particle diffusion coefficient from the dependence of the modulated quantity on the oscillation frequency.

The injected gas is ionized in the peripheral region of plasma and becomes the particle source for electron density. As the source profile is highly peaked in the peripheral region, the particles penetrate into the inner region with a characteristic time delay dominated by the transport process. The dynamics of plasma density is described as the particle diffusion equation using the particle diffusion coefficient D and the flow velocity V ⁵⁾

$$\frac{\partial n}{\partial t} = -\frac{1}{r} \frac{\partial}{\partial r} r\Gamma + S \tag{25}$$

$$\Gamma = -D \frac{\partial n}{\partial r} + V n \tag{26}$$

where n , Γ and S represent the particle density, flux and source, respectively. To apply the numerical method, Eq.(25) is written in a similar form to Eq.(7) as follows

$$\frac{\partial^2 n}{\partial r^2} + \left(\frac{1}{r} + \frac{1}{D} \frac{\partial D}{\partial r} + \frac{V}{D} \right) \frac{\partial n}{\partial r} + \left(\frac{V}{D} \frac{1}{r} + \frac{1}{D} \frac{\partial V}{\partial r} \right) n - i \frac{\omega}{D} n + \frac{S}{D} = 0 \tag{27}$$

These modulation experiments were performed using ohmically heated discharges with a plasma current of 2.5 MA, a toroidal magnetic field of 4.0 T, major and minor radii of 3.28

and 0.90 m, a plasma ellipticity of 1.58, an effective safety factor of 4.5, and a line averaged electron density of $1.8-4.0 \times 10^{19} \text{ m}^{-3}$, using hydrogen as a working gas. (But the ratio of H/(H+D) was about 0.6-0.8, because the deuterium absorbed in the first wall was not fully removed.) The plasma configuration of these discharges can be seen in Fig.1. The modulation frequency of gas puff was scanned from 1 to 7 Hz keeping the injected quantity constant. However, as there is a finite capacity between the gas valve and the vacuum chamber of JT-60U, the supplied gas to the plasma depends on the modulation frequency.

The perturbation quantities of electron density and H-alpha intensity were measured using FIR interferometers and a spectroscopic method using interferometric filter. In Fig.1 the measurement chords of FIR interferometers and H-alpha channels are shown. H-alpha intensity was used as a particle source signal. In the experiments, the bulk electron density (not modulated quantity) was not constant through the scanning of modulation frequency. As the H-alpha intensity has a linear dependence on the electron and neutral particle densities approximately, we used the values of H-alpha intensity divided by the line averaged electron density as the normalized source signal. The measured amplitudes of the density modulation were divided by the normalized source signals and plotted in Fig.2 as a function of the modulation frequency. In the figure, open and solid circles represent the data measured from the U-1 and U-2 chords.

To obtain a solution of Eq.(27), a set of appropriate boundary conditions and profiles of $D(r)$, $V(r)$ and $S(r)$ are necessary. In this analysis, we used two boundary conditions of $\partial n/\partial r=0$ at $r=0$ and $n=0$ at $r=a$ (a is plasma minor radius). In these discharges, the equilibrium density profile $n_0(r)$ was very flat. Using the two measurement chords of the interferometer, the density profiles were fitted in a parabolic form of $n_0(r)=n_0(0)(1-(r/a)^2)^m$. The values of the coefficient m is 0.1 to 0.2. From this result, it was inferred that the inward pinch term is not so large and assumed that $V(r)=0$. The source profile $S(r)$ is considered to peak in the peripheral region. From the review paper of P. C. Stangeby⁶⁾, the half width of the edge source region was estimated to be about 0.05 m. To represent the source profile with this half width, we used a functional form of $S(r)=S(a)(r/a)^{1.5}$.

Using the above mentioned parameters, we calculated the chord integrated density perturbations as a function of the modulation frequency and showed in Fig.3. In the figure, open circle and asterisk symbols represent the measured modulation amplitudes, and solid and dashed lines are the calculated values of U-1 and U-2 chords. In this calculation, we used a profile form of the diffusion coefficient as $D(r)=(D(0)-D(a))(1-(r/a)^2)+D(a)$, where $D(0)$ and $D(a)$ are the center and edge values of the diffusion coefficient. The plot shown in Fig.3 is the best fitted case, where the values of $D(0)/a^2=0.1$ and $D(a)/a^2=0.6 \text{ sec}^{-1}$ are used. Considering a plasma ellipticity of 1.58, it can be estimated that $D(0)=0.1-0.2 \text{ m}^2/\text{sec}$ and $D(a)=0.8 \text{ m}^2/\text{sec}$.

4. Conclusion

Here, we developed a simple numerical method to analyze the general transport equations for source modulation experiments. Using this method, the behavior of several plasma parameters, density, temperature and etc., can be calculated as the response to the source modulation. In this numerical method, the original complex equations are solved as a matrix equation with appropriate boundary conditions. We applied this numerical method to gas puff modulation experiments on JT-60U. From the comparison between the measurement and calculated data, we can estimate that the particle diffusion coefficient is about $0.3 \text{ m}^2/\text{sec}$ in the edge region and $0.1\text{-}0.2 \text{ m}^2/\text{sec}$ in the central region.

ACKNOWLEDGEMENTS

The authors are grateful for many useful discussions with members of the JT-60U team. In particular, we would like to thank Dr. A. Funahashi and Dr. J.C.M. De Haas for their useful comments.

REFERENCES

- 1) G. L. Jahns, S. K. Wong, R. Prater, S. H. Lin, S. Ejima, Nucl. Fusion 26 (1986) 226
- 2) K. W. Gentle, B. Richards, F. Waelbroeck, Plasma Physics and Controlled Fusion 29 (1987) 1077
- 3) K. Krieger, G. Fussmann and the ASDEX Team, Nucl. Fusion 30 (1990) 2392
- 4) K. Nagashima, T. Fukuda, JAERI-M 91-208
- 5) K. Nagashima, T. Fukuda, M. Kikuchi, T. Hirayama, T. Nishitani, H. Takeuchi, Nucl. Fusion 30 (1990) 2367
- 6) P. C. Stangeby, G. M. McCracken, Nucl. Fusion 30 (1990) 1225

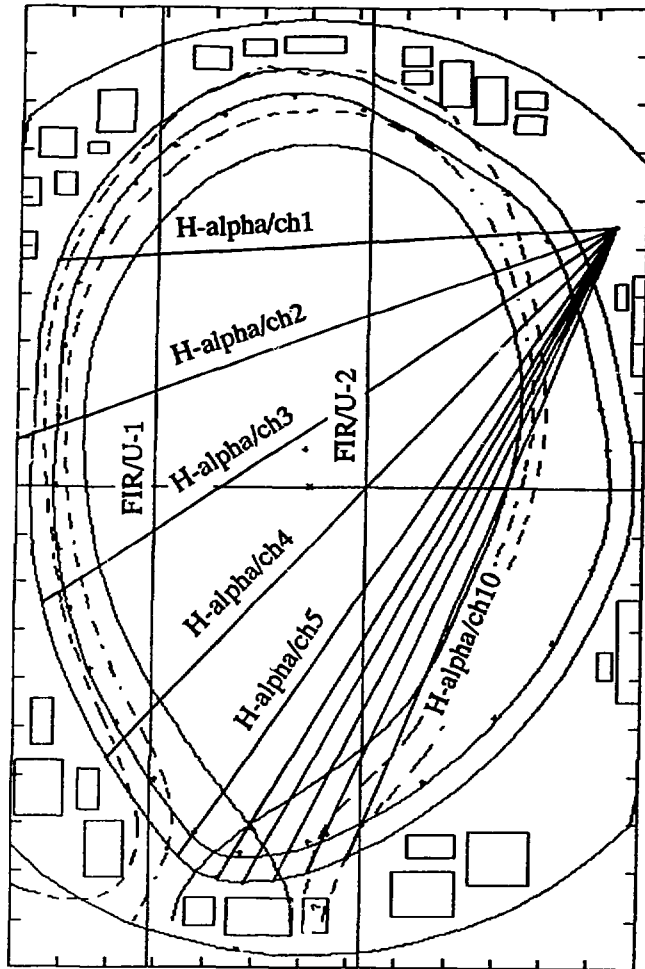


Fig.1 The plasma configuration and the measurement chords of FIR interferometer and H-alpha monitor.

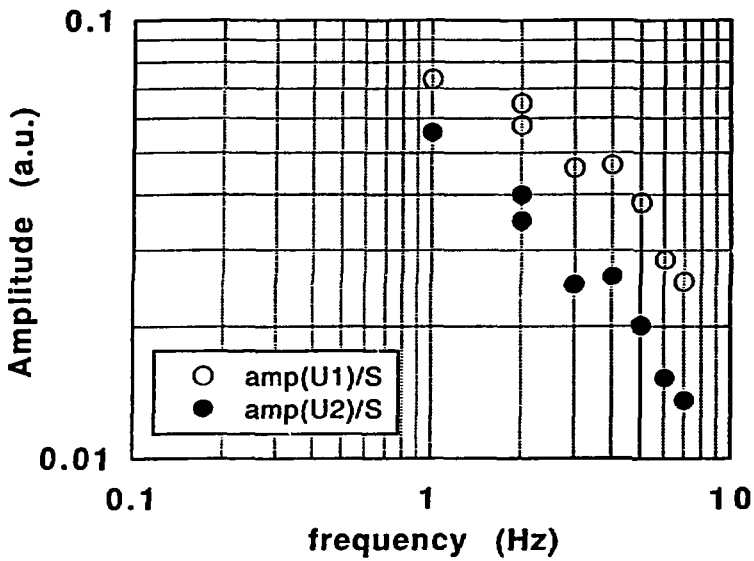


Fig.2 The measured perturbation amplitudes of the chord integrated electron density divided by the normalized source signal. Open and solid circles represent the values obtained from the two measurement chords of U-1 and U-2 ports.

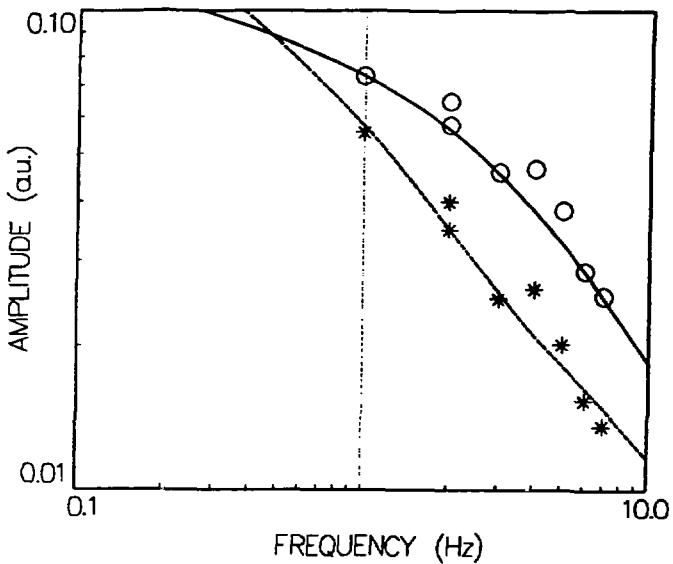


Fig.3 The calculated perturbation amplitudes of the chord integrated electron density. Solid and dashed lines represent the values of U-1 and U-2 chords. (Open circle and asterisk symbols represent the measured amplitudes shown in Fig.2.)

